

# CO<sub>2</sub> and CO vertical distribution in the middle atmosphere and lower thermosphere deduced from infrared spectra

J. VERCHEVAL (\*), C. LIPPENS (\*), C. MULLER (\*), M. ACKERMAN (\*),  
M.-P. LEMAÎTRE (\*\*), J. BESSON (\*\*), A. GIRARD (\*\*), and J. LAURENT (\*\*)

(\* ) *Belgian Institute for Space Aeronomy, B-1180 Brussels, Belgium.*

(\*\* ) *Office National d'Etudes et de Recherches Aérospatiales, Châtillon, France.*

Received 14/05/85, accepted 17/06/85.

**ABSTRACT.** The observation of infrared absorption lines by means of a grille spectrometer on board Spacelab 1 leads to the determination of CO<sub>2</sub> and CO number densities in the low thermosphere and in the middle atmosphere. It is shown how the observational results can be represented by theoretical models based on the interaction processes between solar UV radiation, CO<sub>2</sub>, CO and OH molecules.

*Key words :* CO<sub>2</sub> and CO infrared measurements, modelling.

*Annales Geophysicae*, 1986, 4, A, 2, 161-164.

## INTRODUCTION

During the Spacelab 1 mission, a grille spectrometer operating on the Spacelab pallet has led to observe trace species in the low thermosphere and in the mesosphere by tracking the Sun at sunrise or sunset. Preliminary data on CH<sub>4</sub>, CO<sub>2</sub>, CO, H<sub>2</sub>O, NO and NO<sub>2</sub> molecules have already been published (Lemaître *et al.*, 1984; Lippens *et al.*, 1985; Laurent *et al.*, 1984).

We wish to report here results obtained for the CO<sub>2</sub> and CO molecules in order to compare them with those provided by theoretical models.

## OBSERVATIONAL RESULTS

Several portions of absorption runs were scheduled during the Spacelab 1 mission to observe CO<sub>2</sub> at the highest possible altitudes where its mixing ratio has already been shown to depart from its homospheric values. Figure 1 shows, as an example, the spectrum obtained during event 14 when the sunlight was grazing the Earth at an altitude of 117 km. The region of the strongest absorption lines was chosen near 2360 cm<sup>-1</sup> with a large spectral resolution. The retrieved number densities for two runs are shown in figure 2. The nearly parallel lines represent constant volume mixing ratios from 3 × 10<sup>-8</sup> to 3 × 10<sup>-4</sup>. Event 13 has been studied in detail and the results from two lines are shown. The CO<sub>2</sub> volume mixing ratio follows closely the 3 × 10<sup>-4</sup> value up to 100 km and drops abruptly above this alti-

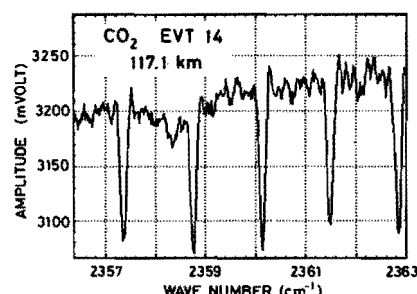


Figure 1  
CO<sub>2</sub> absorption spectrum recorded at sunlight tangent altitude equal to 117 km. See text.

tude by about a factor of 10 over 15 km. These results are in agreement with the mass spectrometric results (Trinks and Fricke, 1978) and give, therefore great confidence in the data obtained with our instrument.

In addition, two absorption runs provided data on carbon monoxide, CO which are also shown on figure 2 by their number density. These values were derived from the P(6) CO line shown in figure 3 at 2119.68 cm<sup>-1</sup>. The observation corresponds to a grazing ray at 92.6 km altitude (sunset) in the northern hemisphere and the dotted line simulates the CO solar line so that the difference between the two curves gives the atmospheric absorption due to CO. This P(6) line is contaminated by ozone absorptions below 60 km precluding a straight-forward CO determination at

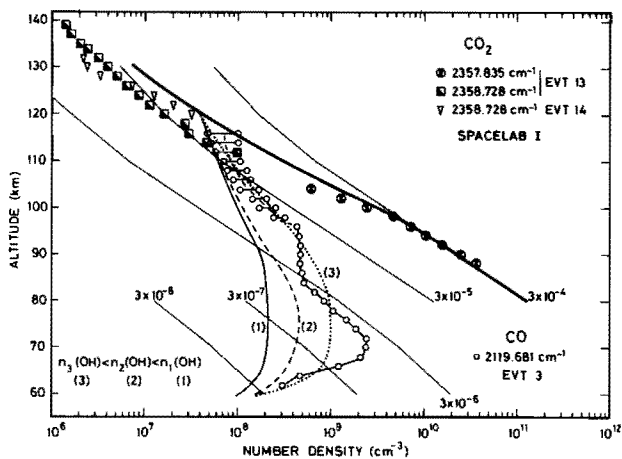


Figure 2  
Number density of CO<sub>2</sub> and CO versus altitude using two different CO<sub>2</sub> absorption lines and the P(6) CO line. The nearly parallel lines represent constant volume mixing ratios from  $3 \times 10^{-8}$  to  $3 \times 10^{-4}$ . The curves (1), (2) and (3) are theoretical profiles of CO number density obtained with the three adopted vertical distributions of  $n(\text{OH})$  shown in figure 5. The solid line is the theoretical profile of CO<sub>2</sub> number density.

lower altitudes. In figure 2, we can detect a large increase of the CO mixing ratio at altitudes where the CO<sub>2</sub> photodissociation by the solar H Lyman  $\alpha$  radiation takes place and where the water vapor H<sub>2</sub>O abundance vanishes abruptly. The CO largest number density is observed near 70 km altitude, close to the H Lyman  $\alpha$  photoproduction peak. Finally, the vertical distribution of carbon monoxide in the mesosphere and thermosphere combined with that of carbon dioxide shows for the first time where these two constituents present equal abundances; our measurements lead to  $115 \pm 5$  km.

In figure 4, the continuous curve shows the profile of CO deduced from the weaker R(2) line observed at sunrise in the southern hemisphere. The R(2) line provided data down to the low stratosphere where a mixing ratio value equal to  $10^{-8}$  is reached at 30 km altitude in agreement with the results obtained from balloon-borne measurements (Farmer *et al.*, 1980; Luisnard *et al.*, 1983). The dotted line represents the profile already shown in figure 2. The comparison between the two observed distributions would indicate a large variability of the mesospheric carbon monoxide and, therefore, the need for more measurements.

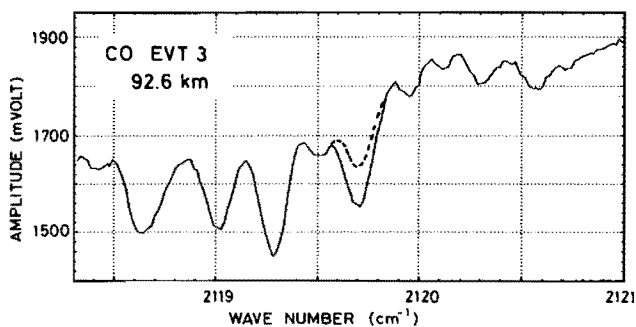


Figure 3  
CO absorption spectrum recorded at sunlight tangent altitude equal to 92.6 km. P(6) line appears at wave number 2119.68 cm<sup>-1</sup>. The dotted line simulates the CO solar line.

THEORETICAL ANALYSIS

Our observations of the CO and CO<sub>2</sub> vertical distribution were compared with theoretical models. These models have been constructed for the 60 to 120 km altitude interval by considering the photodissociation of CO<sub>2</sub> and also the simultaneous reaction of CO with OH molecules leading to reformation of CO<sub>2</sub> ( $\text{CO} + \text{OH} \rightarrow \text{CO}_2 + \text{H}$ ). We have considered steady-state conditions for a solar zenith angle of 75° and atmospheric parameters taken from the standard atmosphere (Nicolet, 1980). In these models, two parameters play a leading role : the eddy diffusion coefficient and the vertical profile of the OH number density.

We have adopted 3 vertical profiles for the hydroxyl number density,  $n(\text{OH})$ , as shown in figure 5. The first one  $n_1(\text{OH})$  is characterized by number densities which are generally the greatest given in the literature with values between  $10^7$  and  $2 \times 10^7$  cm<sup>-3</sup> below 80 km altitude. The second profile,  $n_2(\text{OH})$ , is similar to the first one but with values nearly twice smaller. Finally, a third profile  $n_3(\text{OH})$  was considered with a very abrupt decrease already above 70 km; this third profile is related to the rapid decrease, at the same altitude, of the water vapor mixing ratio which was also observed in the northern hemisphere during sunset and which has been described elsewhere (Lip-pens *et al.*, 1984).

Theoretical profiles were obtained by solving transport and continuity equations. A vertical profile for the eddy diffusion coefficient which provides the best agreement with the observations of CO and CO<sub>2</sub>, was adopted. It leads to a maximum of  $n(\text{CO})$  at about 70 km altitude and a value, at 60 km, which corresponds almost to the photochemical equilibrium conditions between CO and CO<sub>2</sub>.

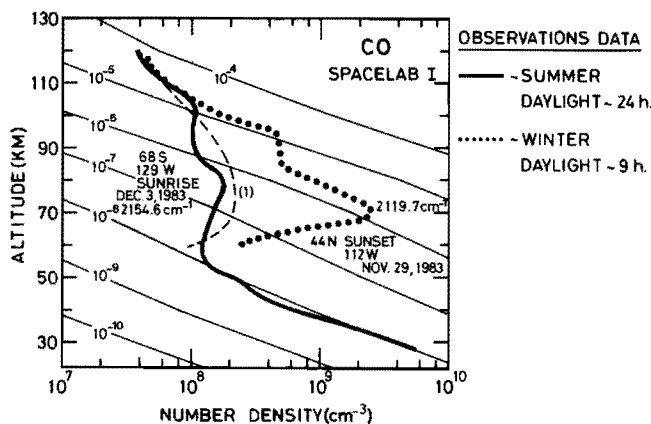


Figure 4  
Carbon monoxide number density versus altitude retrieved from two solar occultation runs, one in the southern hemisphere at sunrise and the other one in the northern hemisphere at sunset. The geographic coordinates of the solar rays tangent points at 50 km altitude are indicated. Two absorption lines were used with different wavenumbers 2154.6 and 2119.7 cm<sup>-1</sup>, respectively. The nearly parallel lines represent constant volume mixing ratios from  $10^{-10}$  to  $10^{-4}$ . The dates of data capture are also given. The dashed line (1) is the theoretical profile of CO number density obtained with the vertical distribution  $n_1(\text{OH})$  shown in figure 5.

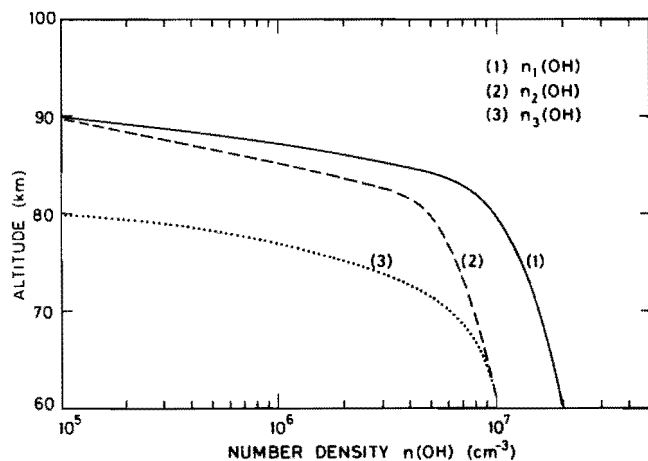


Figure 5  
Vertical distributions of OH number density used in calculations of theoretical profiles of CO abundance. See text.

First, concerning the CO<sub>2</sub> molecule, the solid line shows that there is a perfect agreement up to 100 km and a relatively good one at higher altitudes. The model curves obtained with the 3 adopted vertical profiles of  $n(\text{OH})$  are shown in figure 2. As it can be expected,  $n(\text{CO})$  decreases with an increase of  $n(\text{OH})$ . For instance, a variation of the CO number density, at 75 km, by a factor of 5 indicated by the two extreme curves (1) and (3), corresponds to an OH abundance varying by a factor of 10. It can be seen that the distribution  $n_3(\text{OH})$  corresponding to the smallest values of  $n(\text{OH})$ , is the best one leading to an agreement with the observations. This conclusion gives a support to the measurements of H<sub>2</sub>O already mentioned.

On the other hand, as shown in figure 4, a theoretical agreement with the results of the observations of CO in the southern hemisphere, is obtained with the  $n_1(\text{OH})$  distribution corresponding to the large values of  $n(\text{OH})$ . Two very different vertical profiles of  $n(\text{OH})$  must therefore be considered to reach a theoretical agreement with the observations in the two hemispheres. Such a difference is due to very different solar conditions : summer in the southern hemisphere and winter in the northern hemisphere. As we can see in figure 6, in the southern hemisphere, the sun was almost always above the horizon during the day whereas in the northern hemisphere, daylight had only a duration of about 10 hours. So, water vapor abundances and therefore OH abundances should be very different during the two series of observations with higher values of  $n(\text{OH})$  in the southern hemisphere.

Finally, figure 7 shows the best fit eddy diffusion profiles corresponding to the three adopted values of OH number density.  $D(\text{CO}_2)$  is the diffusion coefficient for CO<sub>2</sub> which plays the leading role above 100 km. It can be seen that there is a satisfactory agreement with the values of the eddy diffusion coefficient obtained by (Allen *et al.*, 1981).

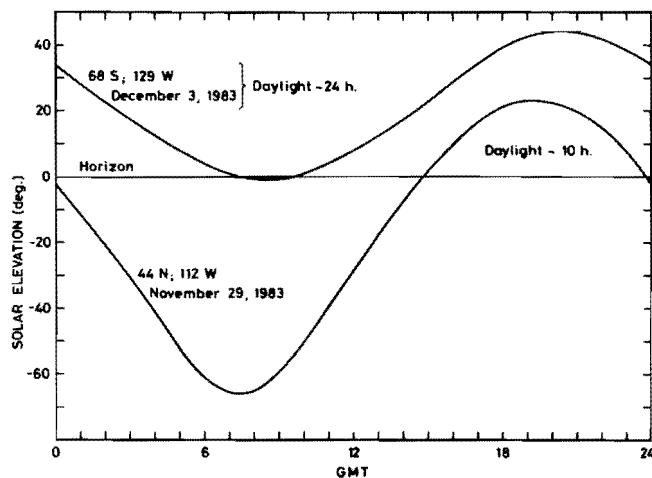


Figure 6  
Solar elevation versus time in hours (GMT) for December 3, 1983 in the southern hemisphere (68 S) and for November 29, 1983 in the northern hemisphere (44 N).

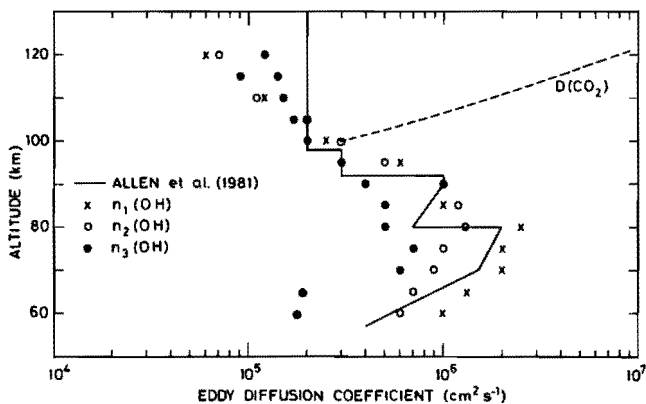


Figure 7  
The best fit eddy diffusion coefficient derived in this paper corresponding to the three adopted vertical profiles of OH number density. The solid line is the eddy diffusion coefficient derived by Allen *et al.* (1981). The dashed curve indicates the diffusion coefficient for CO<sub>2</sub> used in this paper.

CONCLUSION

The results obtained from the grille spectrometer experiment, on the vertical distribution of the CO and CO<sub>2</sub> molecules up to the lower thermosphere, are in agreement with mass spectrometric data in the thermosphere, and balloon-borne instruments in the stratosphere; they can also be represented by theoretical models based on the interaction processes between solar UV radiation, CO<sub>2</sub> and on a set of different values of OH and CO number densities.

Acknowledgements

We wish to thank Prof. M. Nicolet for several helpful discussions.

## REFERENCES

- Allen M., Yung Y. L., Waters J. W., 1981. Vertical transport and photochemistry in the terrestrial mesosphere and lower thermosphere (50-120 km). *J. Geophys. Res.*, **86**, 3617-3627.
- Farmer C. B., Raper O. F., Robbins B. D., Toth R. A., Muller C., 1980. Simultaneous spectroscopic measurements of stratospheric species : O<sub>3</sub>, CH<sub>4</sub>, CO, CO<sub>2</sub>, N<sub>2</sub>O, H<sub>2</sub>O, HCl and HF at northern and southern mid-latitudes. *J. Geophys. Res.*, **75**, 2323-2327.
- Laurent J., Lemaître M.-P., Besson J., Girard A., Lippens C., Muller C., Vercheval J., Ackerman M., 1985. Middle atmospheric NO and NO<sub>2</sub> observed by means of the Spacelab one grille spectrometer. *Nature*, **315**, 126-127.
- Lemaître M.-P., Laurent J., Besson J., Girard A., Lippens C., Muller C., Vercheval J., Ackerman M., 1984. Sample performance of the grille spectrometer. *Science*, **225**, 171-172.
- Lippens C., Muller C., Vercheval J., Ackerman M., Laurent J., Lemaître M.-P., Besson J., Girard A., 1984. Trace constituents measurements deduced from spectrometric observations on board Spacelab. *Adv. Space Res.*, **4**, 75-79.
- Louisnard N., Fergant G., Girard A., Gramont L., Ladobordowsky O., Laurent J., Le Boiteux S., Lemaître M.-P., 1983. Infrared absorption spectroscopy applied to stratospheric profiles of minor constituents. *J. Geophys. Res.*, **88**, 5365-5376.
- Nicolet M., 1980. Etude des réactions chimiques de l'ozone dans la stratosphère. Ed. Institut Royal Météorologique de Belgique, 536 pp.
- Trinks H., Fricke K. H., 1978. Carbon dioxide in the lower thermosphere. *J. Geophys. Res.*, **83**, 3883-3886.